Investigation of the role of the snowpack on atmospheric formaldehyde chemistry at Summit, Greenland

Terra M. Dassau, Ann Louise Sumner, and Stormy L. Koeniger

Department of Chemistry, Purdue University, West Lafayette, Indiana, USA

Paul B. Shepson

Department of Chemistry, Purdue University, West Lafayette, Indiana, USA

Department of Earth and Atmospheric Sciences, Purdue University, West Lafayette, Indiana, USA

Jie Yang and Richard E. Honrath

Department of Civil and Environmental Engineering, Michigan Technological University, Houghton, Michigan, USA

Nicolas J. Cullen and Konrad Steffen

Cooperative Institute for Research in Environmental Sciences, University of Colorado, Boulder, Colorado, USA

Hans-Werner Jacobi, Markus Frey, and Roger C. Bales

Department of Hydrology and Water Resources, University of Arizona, Tucson, Arizona, USA

[1]   Ambient gas-phase and snow-phase measurements of formaldehyde (HCHO) were conducted at Summit, Greenland, during several summers, in order to understand the role of air-snow exchange on remote tropospheric HCHO and factors that determine snowpack HCHO. To investigate the impact of the known snowpack emission of HCHO, a gas-phase model was developed that includes known chemistry relevant to Summit and that is constrained by data from the 1999 and 2000 field campaigns. This gas-phase-only model does not account for the high ambient levels of HCHO observed at Summit for several previous measurement campaigns, predicting approximately 150 ppt from predominantly CH_4 chemistry, which is $\sim$25–50% of the observed concentrations for several years. Simulations were conducted that included a snowpack flux of HCHO based on HCHO flux measurements from 2000 and 1996. Using the fluxes obtained for 2000, the snowpack does not appear to be a substantial source of gas-phase HCHO in summer. The 1996 flux estimates predict much higher HCHO concentrations, but with a strong diel cycle that does not match the observations. Thus, we conclude that, although the flux of HCHO from the surface likely has a significant impact on atmospheric HCHO above the snowpack, the time–dependent fluxes need to be better understood and quantified. It is also necessary to identify the HCHO precursors so we can better understand the nature and importance of snowpack photochemistry.   *INDEX TERMS:* 0322 Atmospheric Composition and Structure: Constituent sources and sinks; 0365 Atmospheric Composition and Structure: Troposphere—composition and chemistry; 1863 Hydrology: Snow and ice (1827); 3367 Meteorolgy and Atmospheric Dynamics: Theoretical modeling

Citation: Dassau, T. M., et al., Investigation of the role of the snowpack on atmospheric formaldehyde chemistry at Summit, Greenland, *J. Geophys. Res.*, *107*(D19), 4394, doi:10.1029/2002JD002182, 2002.
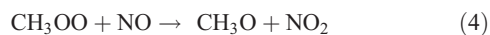
1.   Introduction

[2]   There has recently been considerable interest in air–snow exchange, as chemical species trapped in ice cores contain information regarding long-term changes in atmospheric composition [*Yang et al.*, 1997; *Haan and Raynaud*, 1998; *Stauffer*, 2000]. One of the important concerns about atmospher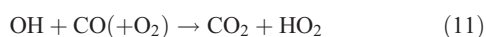ic change relates to the possibility that emissions of trace gases such as NO_x and VOCs may influence the oxidizing power of the atmosphere [*Thompson*, 1995] and thus, indirectly, impact changes in radiatively active gases, such as CH_4. Ice core formaldehyde (HCHO) can be used as a tool for estimating the historical oxidizing capacity of the atmosphere [*Staffelbach et al.*, 1991], i.e., as a proxy for OH radicals, the principal atmospheric oxidant. However, our understanding of factors that control polar atmospheric HCHO and thus air-snow-ice transfer is weak.

[3]   Carbonyl compounds are oxidation products of hydrocarbons, and HCHO is a dominant carbonyl com-

pound produced in this process [*Atkinson et al.*, 1999]. Methane oxidation is the largest source of HCHO in the remote troposphere [*Jaegle et al.*, 2001], as shown in reactions (1)–(5).

$$CH_4 + OH \rightarrow CH_3 + H_2O \qquad (1)$$

$$CH_3 + O_2 \rightarrow CH_3OO \qquad (2)$$

$$CH_3OO + HO_2 \rightarrow CH_3OOH + O_2 \qquad (3)$$

$$CH_3OO + NO \rightarrow CH_3O + NO_2 \qquad (4)$$

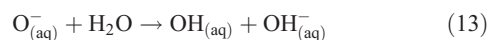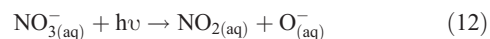$$CH_3O + O_2 \rightarrow HCHO + HO_2 \qquad (5)$$

[4] There is a considerable interest regarding carbonyl compounds in polar regions because the carbonyl compound data in glacial ice core records may be used to infer changes in the composition of the atmosphere [*Staffelbach et al.*, 1991] and they can be important sources and sinks of radicals [*Shepson et al.*, 1996; *Sumner and Shepson*, 1999]. HCHO photolysis, in this environment, is a very important source of HO_x (HO_2 and OH) radicals, as shown in reactions (6a)–(10) and given the rapid HO_2/OH interconversion shown in reactions (9)–(11).

$$HCHO + h\upsilon \rightarrow H_2 + CO \qquad (6a)$$

$$\rightarrow H + CHO \qquad (6b)$$

$$H + O_2 \rightarrow HO_2 \qquad (7)$$

$$CHO + O_2 \rightarrow HO_2 + CO \qquad (8)$$

$$HO_2 + NO \rightarrow OH + NO_2 \qquad (9)$$

$$O_3 + HO_2 \rightarrow 2\,O_2 + OH \qquad (10)$$

$$OH + CO(+O_2) \rightarrow CO_2 + HO_2 \qquad (11)$$

[5] Recent measurements [*Fuhrer et al.*, 1996; *Hutterli et al.*, 1999; *Jacobi et al.*, 2002] show HCHO concentrations in the Summit, Greenland atmospheric boundary layer to be higher than can be predicted by photochemical models, implying that there must be a neglected HCHO source. *Hutterli et al.* [1999] discussed that fresh fallen snow and buried winter snowfall contain HCHO concentrations that are in excess of values that represent equilibrium with the atmosphere, and as a result, the snowpack emits HCHO. In the upper two meters of the snowpack, the HCHO concentration exhibits a maximum just below the surface and then decreases with depth, but with seasonal oscillations, showing winter maxima. HCHO concentrations in the firn air are always higher than in ambient air during the summer [*Fuhrer et al.*, 1996; *Hutterli et al.*, 1999]. It has also been shown that HCHO in surface snow can be photochemically produced, and that this contributes to the large atmospheric HCHO concentrations at the time of polar sunrise, near the Arctic Ocean [*Sumner and Shepson*, 1999; *Sumner et al.*, 2002]. It has been determined that snowpack nitrate ions can photolyze in the snowpack to produce oxidizing radi-

cals, according to reactions (12) and (13) [*Honrath et al.*, 1999, 2000; *Dibb et al.*, 2002].

$$NO_{3(aq)}^- + h\upsilon \rightarrow NO_{2(aq)} + O_{(aq)}^- \qquad (12)$$

$$O_{(aq)}^- + H_2O \rightarrow OH_{(aq)} + OH_{(aq)}^- \qquad (13)$$

These reactions show that NO_x and HO_x radicals are produced in the snowpack condensed phase [*Honrath et al.*, 2000], and since HCHO is produced from OH radical oxidation of a wide variety of organic precursors [*Zhou and Mopper*, 1997], it is likely that HCHO can be photochemically produced in the snowpack. Actinic radiation is known to penetrate $10-20$ cm into the snowpack and thus HCHO will also be photochemically destroyed [*King and Simpson*, 2001; *Peterson et al.*, 2002]. Photochemical processing of HCHO in the snowpack thus complicates the interpretation of ice core HCHO, as it takes several months for deposited species to be buried beneath the photic surface layer [*Peterson et al.*, 2002].

[6] In this paper, we employ field experiments and associated modeling to address the extent of our understanding of atmospheric HCHO above the snowpack at Summit, Greenland, including the nature of air-snow exchange processes and gas-phase photochemistry that may account for the ambient concentrations. Our overall goal is to ascertain the role of the snowpack on atmospheric HCHO chemistry.

2. Experimental Methods

[7] All new measurements presented in this paper were conducted on the Greenland ice sheet at the Summit, Greenland Environmental Observatory (38.4°W, 72.55°N, 3200 m elevation) during the summers of 1999 and 2000. Measurements of gas-phase HCHO were conducted from 27 June to 16 July 1999 and snow samples were collected from 5 June to 3 July 2000 and analyzed at the Purdue laboratory.

2.1. Gas-Phase HCHO Measurements

[8] In 1999, we conducted measurements of gas-phase HCHO, as well as measurements of HCHO in the firn air. Gas-phase HCHO was measured using a flow injection analysis instrument with fluorescence detection [*Fan and Dasgupta*, 1994; *Sumner et al.*, 2002], which was located in a wood enclosure built beneath the snowpack. Briefly, gas-phase HCHO was extracted into water through a 60 cm Nafion membrane diffusion scrubber and was reacted with 1,3-cyclohexanedione and ammonium acetate to produce a fluorescent product (emission at 465 nm). Gas-phase standards were generated from two permeation sources that yielded gas-phase concentrations in the $100-600$ ppt and $1.8-8.0$ ppb range after dilution, and were sampled every 2 hours during the field study. Monomeric HCHO was produced by passing a length of FEP Teflon tubing through solid paraformaldehyde in a heated (40°C) aluminum cylinder. A similar commercial gas-phase standard (Kin-Tek) used α-polyoxymethylene at 60°C to produce HCHO(g). The permeation rate of each device was determined using 2,4-dinitrophenylhydrazine (DNPH) derivatization and HPLC analysis [*Sirju and Shepson*, 1995].

Table 1. Summary of HCHO Measurement Methods for 1993 to 2000

Year	Chemical reaction	Scrubber used	Inlet height, m
1993	1,3-cyclohexanedione	Nafion membrane diffusion scrubber[a]	1
1994	1,3-cyclohexanedione	Nafion membrane diffusion scrubber[a]	1
1996	2,4-pentanedione	Wet effluent diffusion denuder[b]	1
1999	1,3-cyclohexanedione	Nafion membrane diffusion scrubber	1
2000	2,4-pentanedione	Coil scrubber[c]	1.52 or 1.43

[a] *Staffelbach et al.* [1997]. Due to the interference from H_2O_2, HCHO concentrations may be up to 20–30% high.
[b] *Hutterli et al.* [1999].
[c] *Jacobi et al.* [2002].

[9] The inlet line (PFA-Teflon) for gas-phase measurements was positioned 15 meters southeast of the sampling tower, where ambient air was sampled at a height 1 m above the snowpack. A second inlet line was also used during special experiments to allow for alternate sampling from two different locations. A Teflon filter pack (1 μm) was used to remove snow crystals and particulate matter from the ambient air. Data were excluded when snow crystals were found in the ambient sampling line. There is a known interference from H_2O_2 with this method [*Li et al.*, 2001] due to its reaction with cyclohexanedione to form a competing fluorescent product. The sensitivity to HCHO relative to H_2O_2 was determined to be 1:0.035 [*Sumner*, 2001], making the interference only important at low HCHO/H_2O_2 ratios. Because of the high HCHO levels measured at Summit in 1999, and an average H_2O_2 concentration of 1.6 ppb, the hydrogen peroxide interference was determined to be unimportant (ranging from 1 to 11% of the total signal with an average of 4%), compared to the measurement uncertainty. Our instrument has been successfully intercompared with a tunable diode laser (TDL), using the same calibration system, and has been shown to agree very well with a correlation coefficient of 0.95 [*MacDonald et al.*, 1998; *Sumner*, 2001] when the response of our instrument was plotted against the TDL-determined concentration (slope = 0.94 ± 0.03; intercept = 50 ± 40 ppt). For this experiment, however, contributions to the total signal were observed from the inlets, likely from degassing of HCHO from condensation on the inlet walls. This resulted in a high detection limit (3s) of 350 ppt, where the uncertainty in the measurements is approximately +30/−50%. The instrumental precision, based on replicate injections of a gas-phase standard, was ∼10%.

[10] In this paper, we compare computer model output not only to our 1999 measurements, but also to Summit data from 1993, 1994, 1996, and 2000 [*Fuhrer et al.*, 1996; *Hutterli et al.*, 1999; *Jacobi et al.*, 2002]. HCHO measurements for previous years were determined in a similar manner to 1999, as they all involved the reaction of a cyclic dione, in the presence of ammonium ions, to produce a fluorescent product. Table 1 shows a summary of the HCHO measurement methods.

[11] Snowpack interstitial air was sampled using a stainless steel probe, constructed by the Purdue University Jonathan Amy Facility for Chemical Instrumentation. The probe consisted of a 5.1 cm diameter stainless steel cylinder (supported by a perforated aluminum base), through which a length of 6.4 mm Teflon sample line was inserted, terminating at a Teflon filter pack (1 μm) mounted at the bottom of the tube. The probe was positioned by first making a hole in the snowpack with a second stainless

steel tube, of the same dimensions. The probe was then inserted into the bored hole, minimizing the disturbance to the surrounding snowpack. A Type K (Chromel/Alomel) thermocouple was mounted at the tip of the probe and temperatures were monitored with a hand-held Omega digital readout.

2.2. Snow Sampling and Analysis

[12] In 2000, snow samples were collected at Summit and transported to Purdue University for determination of aldehydes, strong acid anions, carboxylic acids, and total organic carbon. Snow samples to be analyzed for total organic carbon (TOC) and aldehydes and ketones were collected in 30 mL and 250 mL glass jars, respectively, with Teflon-lined lids, while snow samples to be analyzed for strong acid anions and carboxylic acids were collected in 100 mL brown, opaque Nalgene high density polyethylene (HDPE) bottles. Sample bottles were precleaned by washing with soap, rinsing, and soaking in Millipore water overnight (repeated twice), followed by three additional rinses. Bottles were tested for leaching of anions, carboxylic acids, and HCHO and were found not to contaminate samples when allowed to remain below 0°C. Millipore water sent to Summit was used to fill identical bottles, which were then frozen and sent back to Purdue where they were analyzed to blank-correct all snow samples. Snow samples were collected from an HDPE tray designed to collect fresh snowfall, and from the surface of the snowpack. All samples remained frozen for the duration of the field study, during transport, and storage at the Purdue laboratory (less than 6 months before analysis).

[13] Snow sample aldehydes and ketones were determined using DNPH derivatization, and separation by high performance liquid chromatography (HPLC) with UV detection at 360 nm (Supelcosil LC-8 column, 25 cm × 4.6 mm ID, Waters 990). The snow samples were melted in a room temperature water bath. Once melted, a 5 mL aliquot of the sample was removed, 0.1 mL acidified DNPH (∼7 mM) was added, the contents were briefly shaken by hand, and reaction was allowed to proceed for 1 hour [*Keiber and Mopper*, 1990] before HPLC injection via a 500 μL sample loop. Gradient elution was conducted by mixing reservoir A (100% acetonitrile) and B (10% acetonitrile in water, pH 2.6), with a constant total flow rate of 1.5 mL min^{-1}. The program profile was as follows (%A/%B): 36/64 for 2 min, increasing to 50/50 over 4 min, constant at 50/50 for 8 min, then to 80/20 over 10 min, and then 100/0 for 20 min.

[14] Liquid-phase carbonyl compound standards were prepared by serial dilution of a HCHO solution standardized using the sodium sulfite method, as described by *Walker* [1964], and using pure aldehydes and ketones. However,

Table 2. Gas-Phase Reactions Used in the HCHO Photochemistry Model, With Rate Constants (second order in cm^3 molecule^{-1} sec^{-1}, first order in sec^{-1} calculated for 255 K, P = 0.67 atm)

Reaction	k(T) or J
OH Reactions	
$OH + CH_4 \rightarrow CH_3OO$	2.39×10^{-15a}
$CH_3CH_3 + OH \rightarrow CH_3CH_2OO$	1.41×10^{-13a}
$HCHO + OH \rightarrow CO + HO_2$	9.30×10^{-12a}
$CH_3CHO + OH \rightarrow CH_3C(O)OO$	1.89×10^{-11a}
$CO + OH \rightarrow HO_2$	1.90×10^{-13a}
$OH + NO_2 \rightarrow HNO_3$	1.60×10^{-11b}
$OH + NO \rightarrow HONO$	3.60×10^{-11b}
$OH + HO_2 \rightarrow H_2O$	1.28×10^{-10b}
$OH + O_3 \rightarrow HO_2$	4.01×10^{-14b}
$HNO_3 + OH \rightarrow NO_3$	2.53×10^{-13b}
$OH + H_2 \rightarrow HO_2$	2.16×10^{-15b}
$CH_3OOH + OH \rightarrow HCHO + OH$	2.11×10^{-12a}
$CH_3OOH + OH = CH_3OO$	4.00×10^{-12a}
$H_2O_2 + OH \rightarrow HO_2$	1.55×10^{-12b}
$CH_3C(O)CH_3 + OH \rightarrow CH_3C(O)CH_2OO$	1.43×10^{-13a}
$C_2H_4 + OH \rightarrow 1.90\ HCHO$	9.00×10^{-12b}
$C_3H_6 + OH \rightarrow HCHO + CH_3CHO$	3.00×10^{-11b}
$CH_3C(O)OONO_2 + OH \rightarrow HCHO + NO_3$	3.00×10^{-14a}
RO$_2$ + NO Reactions	
$CH_3OO + NO \rightarrow NO_2 + HCHO + HO_2$	8.56×10^{-12a}
$CH_3CH_2OO + NO \rightarrow NO_2 + CH_3CHO + HO_2$	1.11×10^{-11a}
$NO + HO_2 \rightarrow NO_2 + OH$	9.33×10^{-12b}
$CH_3C(O)OO + NO \rightarrow NO_2 + CH_3OO$	2.17×10^{-11b}
$CH_3C(O)CH_2OO + NO \rightarrow HCHO + $ $CH_3C(O)OO + NO_2$	8.00×10^{-12c}
RO$_2$ + RO$_2$ Reactions	
$CH_3OO + CH_3OO \rightarrow CH_3OH + HCHO$	2.67×10^{-13a}
$CH_3OO + CH_3OO \rightarrow 2\ HCHO + 2\ HO_2$	1.07×10^{-13a}
$CH_3OO + HO_2 \rightarrow CH_3OOH$	8.09×10^{-12a}
$CH_3CH_2OO + HO_2 \rightarrow CH_3CH_2OOH$	1.30×10^{-12a}
$CH_3CH_2OO + CH_3OO \rightarrow CH_3CH_2OH + HCHO$	6.00×10^{-14d}
$CH_3CH_2OO + CH_3OO \rightarrow CH_3OH + CH_3CHO$	8.00×10^{-14d}
$CH_3CH_2OO + CH_3OO \rightarrow CH_3CHO + 2\ HO_2 + $ $HCHO$	6.00×10^{-14d}
$CH_3OO + CH_3C(O)OO \rightarrow HCHO + HO_2 + CH_3OO$	6.39×10^{-12a}
$CH_3OO + CH_3C(O)OO \rightarrow CH_3C(O)OH + HCHO$	6.39×10^{-12a}
$CH_3CH_2OO + CH_3C(O)OO \rightarrow CH_3CHO + $ $HO_2 + CH_3OO$	5.00×10^{-12a}
$CH_3CH_2OO + CH_3C(O)OO \rightarrow CH_3CHO + $ $CH_3C(O)OH$	5.00×10^{-12a}
$CH_3C(O)OO + HO_2 \rightarrow CH_3C(O)OOH$	2.27×10^{-11b}
$2\ CH_3C(O)OO \rightarrow 2\ CH_3OO$	2.06×10^{-11a}
$CH_3C(O)CH_2OO + HO_2 \rightarrow CH_3C(O)CH_2OOH$	9.00×10^{-12e}
RO$_2$ + NO$_2$ Reactions	
$CH_3OO + NO_2 \rightarrow CH_3OONO_2$	7.50×10^{-12a}
$CH_3CH_2OO + NO_2 \rightarrow CH_3CH_2OONO_2$	8.80×10^{-12a}
$CH_3C(O)OO + NO_2 \rightarrow CH_3C(O)OONO_2$	1.39×10^{-11a}
$HO_2 + NO_2 \rightarrow HO_2NO_2$	5.90×10^{-12b}
RO$_2$NO$_2$ Reactions	
$CH_3OONO_2 \rightarrow CH_3OO + NO_2$	1.14×10^{-2a}
$CH_3CH_2OONO_2 \rightarrow CH_3CH_2OO + NO_2$	1.46×10^{-2a}
$CH_3C(O)OONO_2 \rightarrow CH_3C(O)OO + NO_2$	1.51×10^{-7a}
$HO_2NO_2 \rightarrow HO_2 + NO_2$	5.40×10^{-4e}
Misc. Reactions	
$O_3 + NO \rightarrow NO_2$	8.36×10^{-15e}
$O(^1D) \rightarrow O_3$	$5.69 \times 10^{+8b}$
$O(^1D) \rightarrow 2\ OH$	$7.47 \times 10^{+6b}$
$HO_2 + O_3 \rightarrow OH$	1.55×10^{-15b}
$2\ HO_2 \rightarrow H_2O_2$	2.42×10^{-12b}
$NO_2 + O_3 \rightarrow NO_3$	8.06×10^{-18b}
$NO_2 + NO_3 \rightarrow N_2O_5$	1.50×10^{-12b}
$N_2O_5 \rightarrow NO_2 + NO_3$	1.31×10^{-4e}
$NO + NO_3 \rightarrow 2\ NO_2$	2.92×10^{-11b}
Photolysis Reactions	
$NO_2 \rightarrow NO + O_3$	Variable[f]
$O_3 \rightarrow O(^1D)$	Variable[f]
$HONO \rightarrow OH + NO$	Variable[f]
$HCHO \rightarrow 2\ HO_2 + CO$	Variable[f]
$HCHO \rightarrow H_2 + CO$	Variable[g]

Table 2. (continued)

Reaction	k(T) or J
$NO_3 \rightarrow NO_2 + O_3$	Variable[h]
$NO_3 \rightarrow NO$	Variable[h]
$CH_3CHO \rightarrow CH_3OO + HO_2 + CO$	Variable[f]
$CH_3C(O)CH_3 \rightarrow CH_3OO + CH_3C(O)OO$	Variable[f]
$CH_3OOH \rightarrow OH + HO_2 + HCHO$	Variable[f]
$H_2O_2 \rightarrow 2\ OH$	Variable[f]
Emissions	
$HONO$	Variable[i]
$HCHO$	Variable[j]
H_2O_2	Variable[j]
Depositions	
HNO_3	8.00×10^{-5h}
N_2O_5	8.00×10^{-5h}
$HCHO$	Variable[j]
H_2O_2	Variable[j]

[a] *Atkinson et al.* [1999].
[b] *DeMore et al.* [1997].
[c] *Sehested et al.* [1998].
[d] *Villeneuve and Lesclaux* [1996].
[e] *Atkinson et al.* [1997].
[f] Curve fitting and interpolation of *Yang et al.* [2002] values.
[g] Scaling of JHCHO1 from *Simpson et al.* [2002] equations and JHCHO2.
[h] Scaled from or based upon the *Michalowski et al.* [2000] NO_3 and NO_2.
[i] Simulation of ambient concentrations.
[j] *Jacobi et al.* [2002].

HCHO was the only compound detected in snow above the method detection limit (5×10^{-8} M). The coefficient of variance for the method, as determined by analyzing repeated samples was 7%; whereas, for the triplicate sample analysis (which includes sample concentration variability), it was 44%.

[15]   Strong acid anions (F^-, Cl^-, NO_3^-, and SO_4^{2-}), and carboxylic acid anions (lactate, acetate, propionate, formate, methylsulfonate, and oxalate) were determined in melted snow samples using ion chromatography (Dionex DX-500 IC, 200 μL sample loop). Samples were separated using a Dionex AS11 separation column and an AG11 guard column using a gradient program increasing from 0.2 mM NaOH to 38.25 mM NaOH over 20 min at a flow rate of 2 mL min^{-1}. Anions were detected via conductivity using a Dionex ASRS-Ultra II micromembrane suppressor in autorecycle mode. Calibrations were achieved by serial dilution of freshly prepared acid and anion standards.

[16]   Snow-phase total organic carbon (TOC) was measured using an automated Shimadzu TOC-5000A analyzer with an ASI-5000A autosampler. TOC was calculated as the difference between measured total carbon and inorganic carbon, detected as CO_2 via nondispersive infrared absorption. The instrument determines total carbon by combustion of all organic material to CO_2 with the use of platinum on alumina catalyst at 680°C. Inorganic carbon was measured by acidifying all carbonates to CO_2 using 25% phosphoric acid. Solutions of potassium hydrogen phthalate and sodium carbonate/bicarbonate were used for total carbon and inorganic carbon standards, respectively. All analyzed samples were well above the instrument limit of detection of 50 μg L^{-1} for total carbon and 30 μg L^{-1} for inorganic carbon. The coefficient of the variance for the TOC measurements was 13% based on replicate analysis of the same sample and 50% based on triplicate sampling, which includes snowpack concentration variability and sampling artifacts.

Table 3. Initial Gas-Phase Concentrations for Model Species

Species	Initial concentration	Constant/variable
CH_4	1.8 ppm	Constant
CH_3CH_3	713 ppt	Constant
H_2	580 ppb	Constant
CO	114 ppb	Constant
O_3	40 ppb	Constant
$CH_3C(O)CH_3$	1.2 ppb	Constant
H_2O_2	452 ppt	Variable
HCHO	100 ppt	Variable
CH_3CHO	8 ppt	Variable
NO	7 ppt	Variable
NO_2	40 ppt	Variable
NO_3	10 ppt	Variable
HONO	2 ppt	Variable
C_2H_4	9 ppt	Constant
C_3H_6	6 ppt	Constant

2.3. Gas-Phase Photochemistry Model

[17] The zero-dimensional box model of atmospheric photochemistry was developed using the Chemical Reactions Modeling System (CREAMS) which improved on previous models [e.g., *Neftel et al.*, 1995] by constraining the model given time varying, measured gas-phase concentrations for many species on the basis of observations during the 1999 and 2000 field campaigns. Specifically, we included a flux of HONO from the snowpack as shown to occur by *Honrath et al.* [2002], in which the magnitude of the time varied flux (with a cosine dependence following radiation) was altered until the model simulated NO, NO_2, and HONO agreed with observations [*Dibb et al.*, 2002; Honrath et al., unpublished data]. The model incorporates methane, ethane, ethene, propene, and acetone chemistry and includes time varying photolysis rate constants for NO_2, O_3, NO_3, HONO, HCHO, H_2O_2, CH_3OOH, $CH_3C(O)CH_3$, and CH_3CHO, which were calculated based on radiation measurements [*Yang et al.*, 2002]. Adding the chemistry of

other organic molecules measured at Summit (Swanson et al., unpublished data), such as methanol, at the highest measured concentration, does not contribute significantly to HCHO production. The 65 reactions included in this model are shown in Table 2, with the appropriate rate constants, calculated from Arrhenius expressions (where available) for T = 255K and P = 0.67 atm. Initial concentrations for simulated species are listed in Table 3. In general, species that were not produced in the model and have long lifetimes were input at constant concentrations; those that were reaction products and/or short-lived were allowed to vary.

3. Results and Discussion

3.1. Ambient HCHO Measurements

[18] Ambient air HCHO concentrations from 3 to 18 July 1999 are presented in Figure 1. H_2O_2 data are also presented as H_2O_2 is a product of HCHO photolysis from the HO_2 self-reaction and is thus related to HCHO. The range of observed HCHO concentrations was 300–1500 ppt, which is, on average, higher than previous measurements. Previous investigators reported HCHO concentrations in the range of 50–200 ppt [*Jacobi et al.*, 2002], 200–300 ppt [*Hutterli et al.*, 1999], and 200–600 ppt [*Fuhrer et al.*, 1996]. Although the estimated uncertainty in the 1999 measurements is relatively high, we believe the data reflect a real interannual difference in HCHO concentrations. As shown in Figure 1, H_2O_2 and HCHO concentrations appear to be correlated. Although both species exhibit a pronounced diel cycle early in this measurement period, the diel cycle is not consistently present. *Fuhrer et al.* [1996] and *Hutterli et al.* [1999] did not observe a diel cycle, but the most recent gas-phase measurements [*Jacobi et al.*, 2002] do indicate the presence of a diel cycle. On 3, 5, and 8 July, a pattern is evident that shows HCHO reaching a maximum concentration in the late morning/early afternoon. In Figure 2, these data are plotted along with radiation and
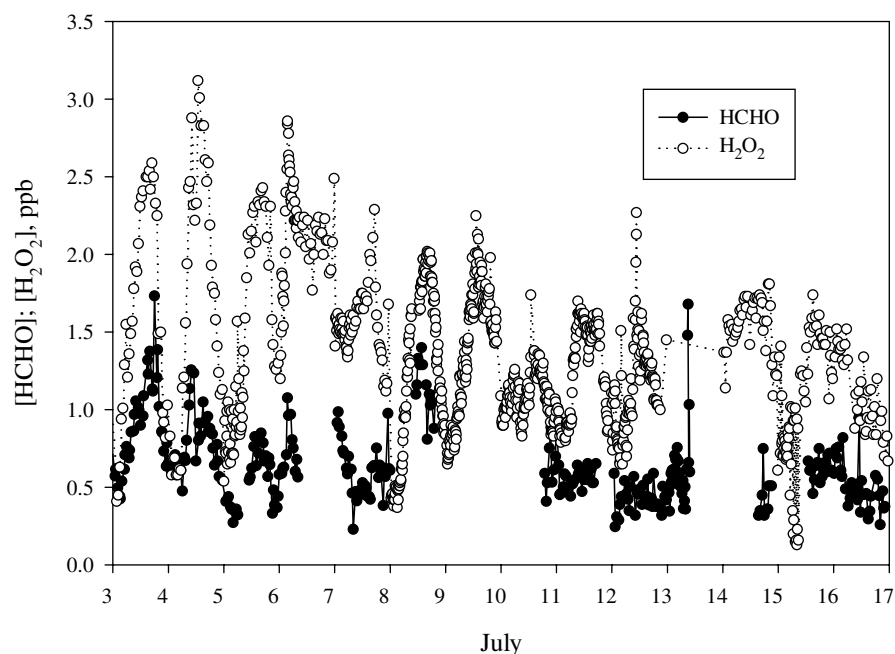

Figure 1. Ambient HCHO and H_2O_2 mixing ratios (in ppb) from 3 to 17 July 1999.
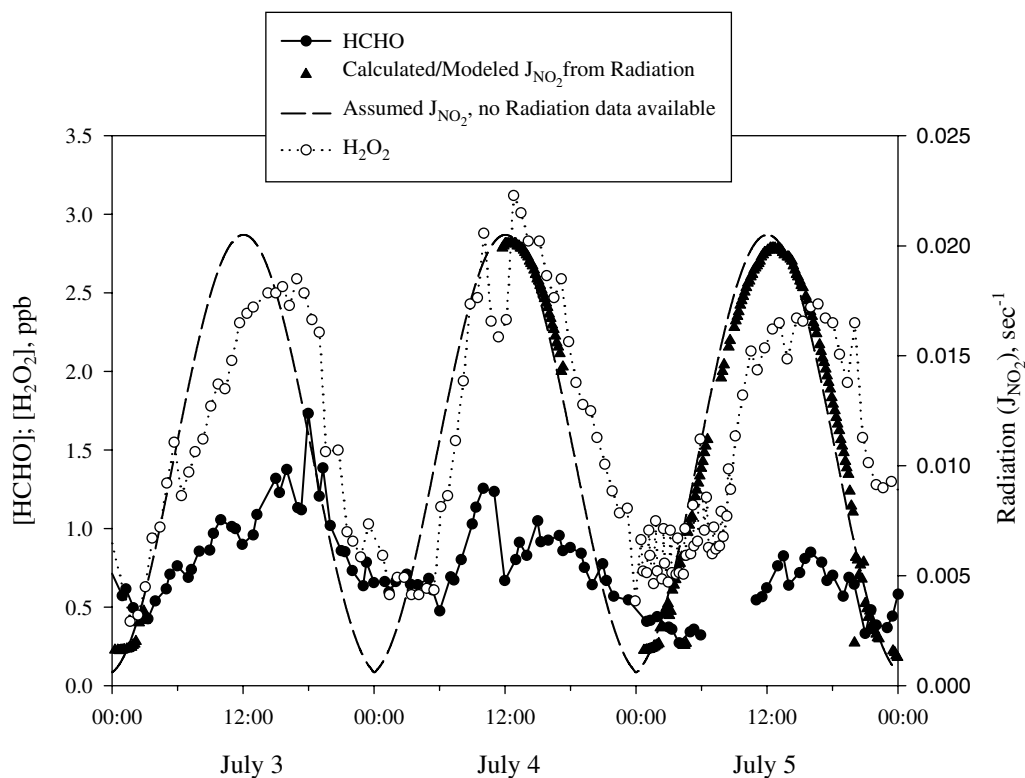
Figure 2. Ambient HCHO and H_2O_2 mixing ratios (in ppb) from 3 to 6 July 1999. Modeled relative radiation (scaled to measured radiation) is also plotted as J_{NO2}. Where measured radiation is not available, a best-fit estimate of the data is presented (dashed line).

H_2O_2 to show that their variability has a similar pattern to radiation (and temperature). NO_2 photolysis rate constants (J_{NO2}), calculated from radiation measurements [*Yang et al.*, 2002], are shown to represent radiation. On average, for these days, both HCHO and H_2O_2 maximize after solar noon.

[19] Using all available data for this time period, the 1999 HCHO concentrations were plotted against temperature and radiation measurements to determine the extent of their correlation. It was found that ambient HCHO correlated with both variables with correlation coefficients (r^2) of 0.50. It is important to note that, while the HCHO observations are high relative to those from other years, the same is true for H_2O_2. Previous investigations found ambient H_2O_2 at levels typically between 0.2 and 1.2 ppb, considerably lower than those shown in Figure 2 [*Fuhrer et al.*, 1996; *Jacobi et al.*, 2002]. The large concentration of H_2O_2 (in 1999) and correlation with HCHO is consistent with the fact that HCHO photolysis will be an important source of HO_2 radicals, as shown by reaction (14).

$$HO_2 + HO_2 \rightarrow H_2O_2 + O_2 \qquad (14)$$

3.2. Snowpack HCHO Processing and Snow Composition

[20] An important issue for interpretation of both gas-phase HCHO, as well as ice core concentrations is that of postdepositional photochemical processing. *Haan et al.* [2001] propose that photolysis of HCHO is a source of the photochemical production of CO from sunlit snow. The recent data by *Couch et al.* [2000] and *Burkhart et al.*

[2002] imply that the HCHO−methylene glycol equilibrium in snow lies to the unhydrated side. If this is the case, it will be photolyzed on a timescale that is short (<1 day) relative to its burial time (∼several months). As discussed by *Fuhrer et al.* [1996], *Sumner and Shepson* [1999], and *Sumner et al.* [2002], HCHO could be photochemically produced in the snowpack as well. Indeed, if HCHO can be photochemically destroyed in the surface snowpack condensed phase on timescales comparable to the gas-phase lifetime (i.e., a few hours), some photochemical production is necessary to sustain the observed condensed-phase concentrations.

[21] To examine the potential for photochemical production of HCHO in the snowpack, firn air measurements in 1999 were obtained with alternating ambient measurements to examine the relationship between snowpack gas-phase HCHO concentrations and the ambient concentrations above. The snowpack temperature was also measured from the tip of the snow probe sampling the firn air. To isolate the radiation variable, we used a 1 m × 2 m rectangular piece of Styrofoam to shade the snow surface. In this experiment, the Styrofoam was suspended approximately 15 cm above the snowpack surface, to shade the snowpack. This allowed for the control of radiation penetrating into the snowpack, without significantly affecting snowpack temperature or ventilation. In this experiment, as shown in Figure 3, ambient HCHO concentrations were constant, simplifying the analysis of the radiation impact. During this experiment, the HCHO concentrations in the firn air were greater (∼5 times) than those in the ambient air aloft, implying a flux to the atmosphere throughout the day, in accord with previous
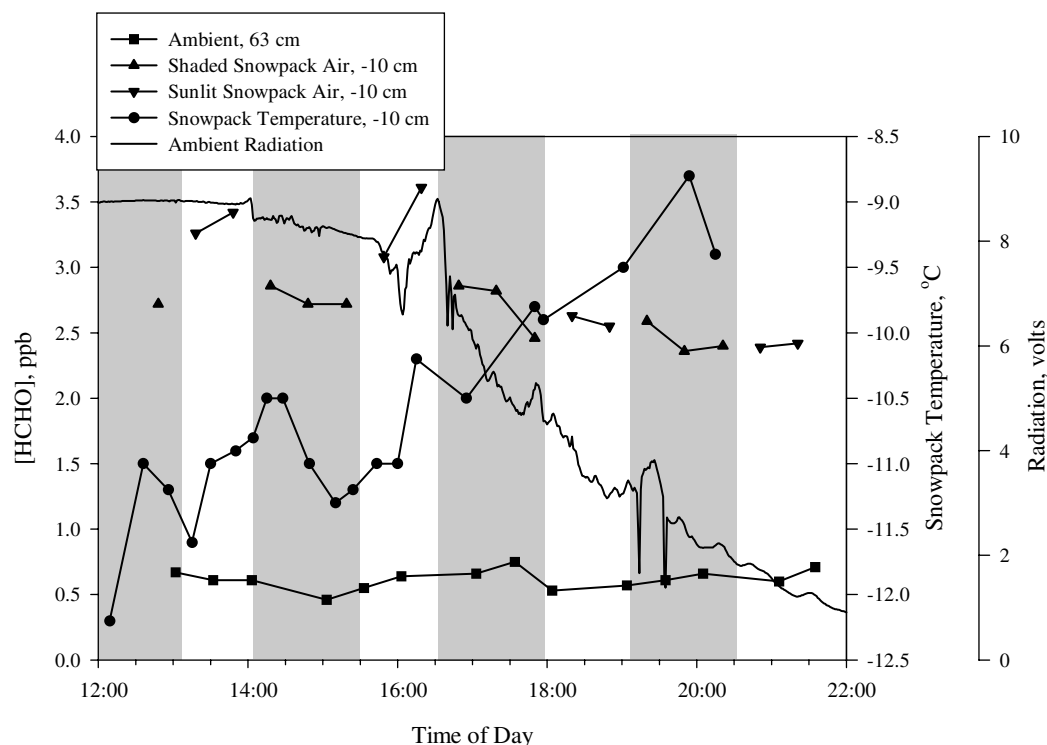
Figure 3. Firn air shading experiment, 15 July 1999. This plot shows the effect of shading and unshading the snow surface on snowpack air at -10 cm. Ambient HCHO (in ppb) is shown by the squares, and snowpack air HCHO (in ppb) is shown by the triangles (inverted triangles depict unshaded snowpack air and upright triangles depict shaded snowpack air). Radiation signal decreases throughout the measurement period and is shown by the solid line, whereas snowpack temperature (in °C) increases and is shown by the circles.

observations [*Fuhrer et al.*, 1996; *Hutterli et al.*, 1999; *Sumner and Shepson*, 1999; *Jacobi et al.*, 2002]. In the early afternoon, when radiation was high, covering and uncovering the snowpack produced a significant result: HCHO levels were higher when the snowpack was exposed to ambient radiation and decreased when this radiation was removed. Thus radiation induced a larger snowpack efflux of HCHO to the atmosphere. Comparable results were also obtained in 2000 for similar firn air experiments. At lower radiation levels (i.e., after 1800), this effect was not apparent. An interesting note is that the snowpack temperature increased throughout this experiment, while the covered snowpack air concentrations were slowly decreasing. Thus during these experiments, if thermal desorption were the cause of the short-timescale changes in the interstitial air HCHO concentrations, that desorption would have to occur from other depths (presumably lower) and diffuse to the inlet depth. The result shown in Figure 3 is more likely caused by snowpack photochemical production, a conclusion that is consistent with the results of *Sumner et al.* [2002] for Alert, Nunavut.

[22] HCHO and other carbonyl compounds can be produced from condensed-phase OH oxidation of organic matter, where the OH radicals may be produced from reactions (12) and (13). To better understand the chemistry, it is necessary to understand the composition of the organic material in the snow. With this in mind, we conducted measurements of the total organic carbon content of snow and determined the concentrations of snow-phase carboxylic acids and HCHO. On 6 June 2000, a sample was obtained immediately after a snow event. This is of interest, as the carbon in this snow will result mainly from what is incorporated in snowfall, rather than from dry deposition. For this particular snow sample, we found a total organic carbon content of 1.85 mg C L^{-1} and an inorganic carbon content of 1.08 mg C L^{-1}. Of that organic carbon, HCHO accounted for 1.93%, while the carboxylic acids and MSA accounted for 1.76% (1.18% acetate, 0.32% propionate, 0.21% formate, 0.03% MSA, 0.02% lactate). Thus, we can account for only ~4% of the total organic carbon content. This is the first attempt to account for the snowpack organic carbon budget at Summit. *Twickler et al.* [1986] measured organic carbon levels in the Greenland snowpack between 0 and 150 cm (~40 km southwest of Dye 3, 44.87°W, 65.01°N). Their average TOC concentration was 0.11 mg L^{-1}, with a range of $0.03-0.32$ mg L^{-1}, lower than our measurements. It is clear that in order to understand the condensed-phase organic chemistry that leads to production of a wide variety of photochemical oxidation products, additional work is needed to characterize the nature and source of the organic matter in the snowpack. As in the gas phase, the snowpack could contain larger organic materials that can oxidize to produce HCHO. Large alkanes, aldehydes, alcohols, aromatics, and fulvic acids have been observed in Antarctic snow [*Desderi et al.*, 1998; *Cincinelli et al.*, 2001; *Calace et al.*, 2001] and other high alpine sites
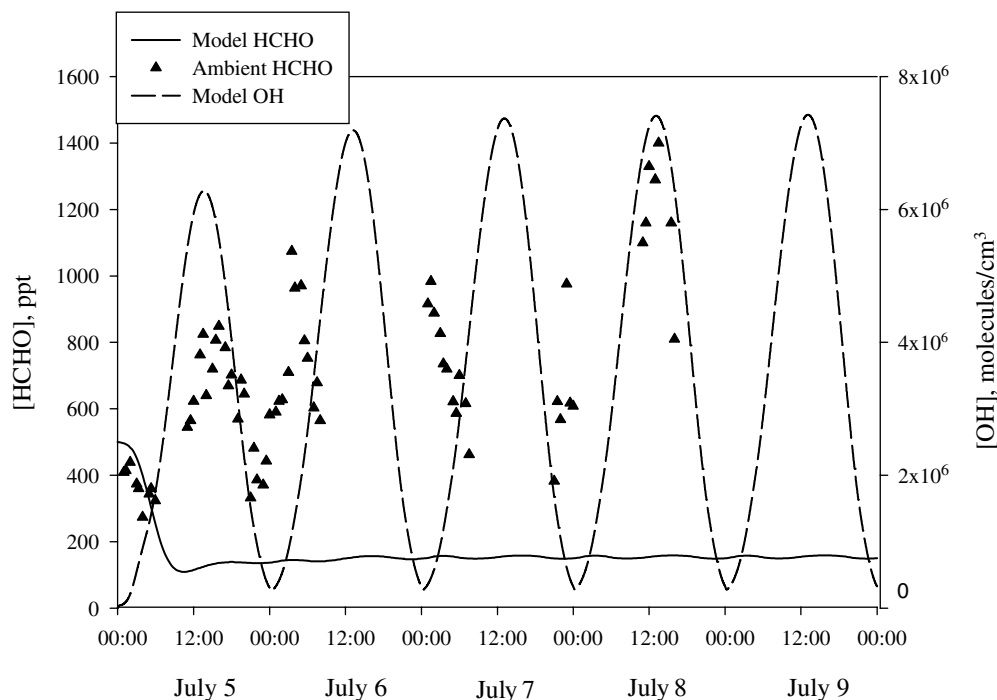
Figure 4. Five-day model simulation of HCHO at Summit, Greenland, 5 to 10 July 1999. Model output (solid line) is compared to 1999 HCHO mixing ratios (triangles, in ppt). Simulated OH is plotted as the dashed line (in molecules cm^{-3}).

[*Grollert and Puxbaum*, 2000], so it is reasonable to assume that significant HCHO precursors are also present in the snowpack at Summit.

3.3. Model Simulations

3.3.1. Base Photochemical Model

[23] To evaluate our understanding of Summit HCHO chemistry, we conducted a 5-day simulation corresponding to conditions during 5 to 9 July 1999 (chosen because of full data coverage), as shown in Figure 4. As discussed by *Dibb et al.* [2002], HONO levels are surprisingly high in the snowpack air (∼80 ppt) as compared to ambient concentrations (∼5–20 ppt, generally) and have a significant impact on ambient HO$_x$ levels [*Yang et al.*, 2002] when released into the atmosphere. The simulated OH levels, shown in Figure 4, demonstrate a solar noon peak of ∼7 × 10^6 molecules cm^{-3}. These OH concentrations are higher than previously expected, but agree with calculations of *Yang et al.* [2002], who predict an OH maximum of 5 × 10^6 to 8 × 10^6 molecules cm^{-3}. As shown, the model yields a nearly constant HCHO concentration after ∼1 day. The gas-phase-only model results in HCHO concentrations of 148–156 ppt. The observed 1999 gas-phase concentrations were as much as 5 times greater than those predicted by the model, assuming only gas-phase photochemical production. To thoroughly examine the model measurement comparison, we also present in Figure 5 all previously reported HCHO measurement data for Summit, shown as diel average concentrations. For each field campaign, the diurnally averaged atmospheric HCHO concentration data for the full measurement period are plotted. Modeled HCHO is lower than measured for all but the 2000 campaign (even without a snowpack flux of HCHO; for

2000, observed average [HCHO] = 125 ± 34, (N = 41) during the 1200–1300 time period), and are significantly lower than most of the 1993, 1994, and 1999 HCHO data. Specifically, the model simulation indicates a noon [HCHO] = 155 ppt and the observed diurnal average concentrations and variability (1s) are 404 ± 52 ppt (N = 13), 321 ± 89 ppt (N = 37), and 751 ± 290 ppt (N = 8), respectively for 1993, 1994, and 1999 between 1200 and 1300. The 1996 observed diurnal average is significantly higher than the model at some points, but not throughout the day (noon average = 215 ± 47 ppt, N = 5). These results imply that emission from the snowpack may significantly impact gas-phase concentrations. If gas-phase HCHO concentrations are determined in part by emission of various species from the snowpack, there could be significant interannual variability, at a minimum, because of variations in the HCHO flux, and the HONO flux. The HONO flux (which largely determines surface layer OH) will be dependent on the deposition rates for HNO$_3$ and particle/snow NO$_3^-$ [*Honrath et al.*, 2000]. The base model, which does not include a contribution to HCHO from the snowpack, does not exhibit any diel cycle. The lack of a diel cycle is consistent with the 1996 data [*Hutterli et al.*, 1999] and the 10 to 17 July 1999 data. The 2000 data [*Jacobi et al.*, 2002] shows a diurnal variation in HCHO, which maximizes in the morning. This is not evident in the gas-phase base model and implies that if there is a diurnal cycle in gas-phase HCHO, it is not caused by known gas-phase photochemistry.

[24] Previous models predicted a summer, noontime HCHO concentration of ∼90 ppt, and attributed the discrepancy between model prediction and ambient concentration to an underestimate of the HCHO sources [*Neftel et*
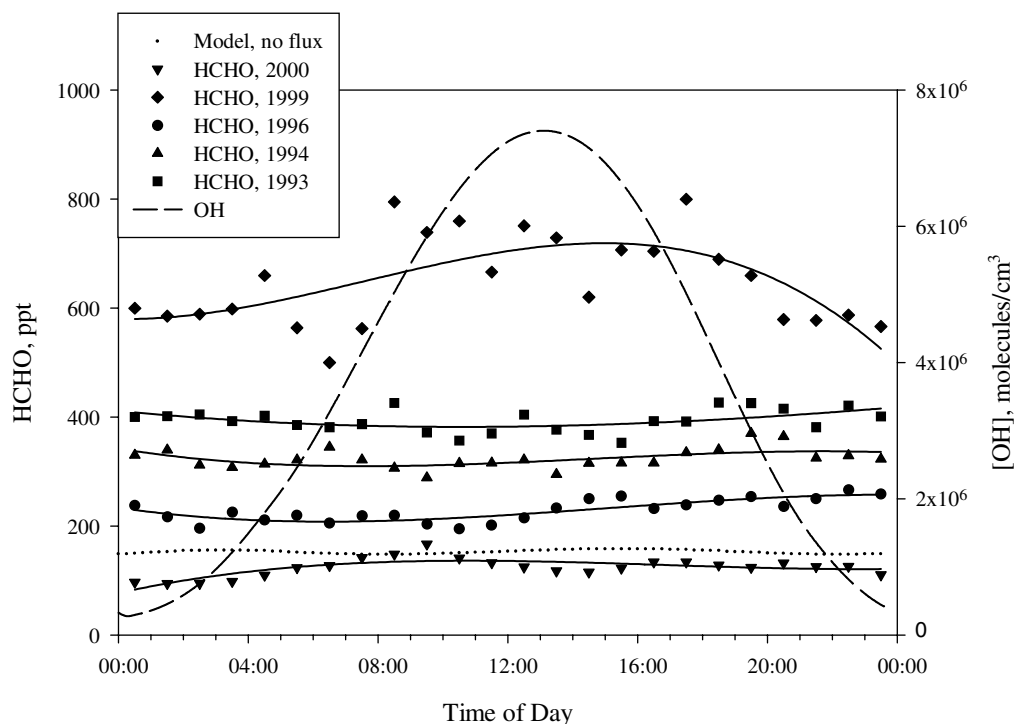
Figure 5. Comparison of modeled HCHO to 5 years of ambient data. Modeled HCHO is shown in this plot for 7 July 1999 (small dots). These values are compared to diel averages for all 5 years of HCHO data. The curves that correspond to each data set are cubic polynomial fits. In addition, OH (in molecules cm^{-3}) is shown for comparison.

al., 1995]. Our updated model predicts higher levels of gas-phase HCHO, at 156 ppt for the same season and time. The difference is largely due to the greater OH concentrations in this model, resulting from inclusion of HONO emission from the snowpack, and also to more efficient conversion of CH_3OO to CH_3O via NO (reaction (4)), resulting from NO_x emissions from the snowpack. To examine the relative importance of various HCHO sources, we calculated the rates of each reaction that produced HCHO in our model, from noon to 1300 on 7 July 1999, including the role of input via the surface flux. The results are shown in Table 4. Clearly CH_3OO, from the reaction of CH_4 + OH (reaction (1)), is the most important HCHO source in the model. Although CH_3OOH (methylhydroperoxide) oxidation is important, this species is also produced largely from CH_4 oxidation.

3.3.2. Snowpack Flux Estimates

[25] It is now well known that HCHO can efflux from the snowpack, particularly from fresh fallen snow [*Hutterli et al.*, 1999; *Houdier et al.*, 2002], and the data in Figure 3 suggest that snowpack photochemistry may enhance this flux. These two facts imply that the snowpack could be an important source of ambient HCHO, and may account for the difference in measurement and model predictions. Thus, we wish to use the measured HCHO fluxes from the snowpack to examine the effect of this additional HCHO source on gas-phase HCHO.

[26] *Hutterli et al.* [1999] reported HCHO fluxes ranging from 1.4×10^{12} to 8.8×10^{12} molecules m^{-2} sec^{-1}, as determined during the summer of 1996, based on five snow-phase HCHO gradient measurements conducted on different

dates and times. However, the calculated fluxes were lower limits, and their best estimate average snowpack HCHO flux, determined via modeling, for June at Summit, Greenland was reported as 1.0×10^{13} molecules m^{-2} sec^{-1}. *Jacobi et al.* [2002] found the HCHO flux to be diurnally varying, and both emission and deposition of HCHO and H_2O_2 were shown to occur from and to the snowpack. This is consistent with the results of *Grannas et al.* [2002]. In

Table 4. Relative Production Rates for HCHO from the Gas-Phase Model Between Solar Noon and 1300 (top)

Sources of HCHO from model output	
Reactants	% of total HCHO production
CH_3OO + NO	78.7
CH_3OOH + OH	5.52
C_2H_4 + OH	5.34
CH_3OOH + hv	4.13
C_3H_6 + OH	3.29
$CH_3C(O)CH_3$ + OH	2.33
CH_3OO + CH_3OO	0.39
CH_3OO + $CH_3C(O)OO$	0.26
PAN + OH	0.06
CH_3OO + CH_3CH_2OO	0.00

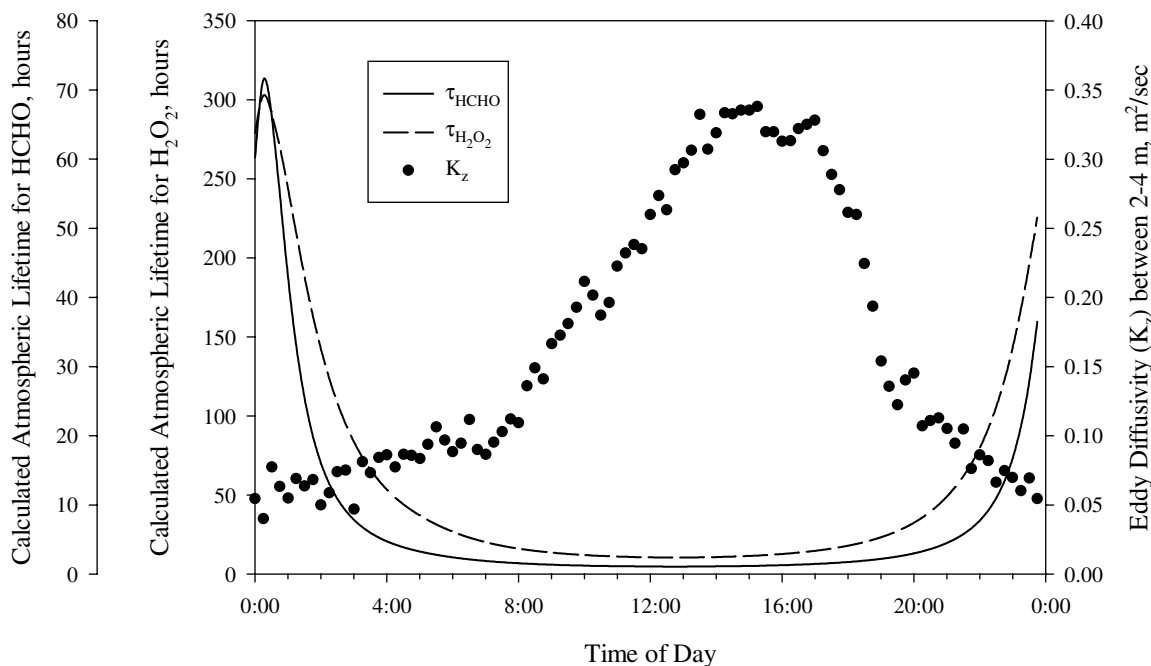| Sources of CH_3OO from model output	
Reactants	% of total CH_3OO production
CH_4 + OH	77.0
CH_3OOH + OH	10.3
$CH_3C(O)OO$ + NO	7.07
$CH_3C(O)CH_3$ + hv	5.28
CH_3CHO + hv	0.36
2 $CH_3C(O)OO$	0.06
CH_3CH_2OO + $CH_3C(O)OO$	0.00

Figure 6. Diurnal variation of atmospheric lifetime and eddy diffusivity. Calculated atmospheric lifetime is plotted for HCHO (solid line, in hours) and H_2O_2 (dashed line, in hours). The points represent the eddy diffusivity calculated between 2 and 4 m (in $m^2\ sec^{-1}$).

addition, *Perrier et al.* [2002] propose that photochemical production of HCHO can occur within the snowpack causing an immediate release of HCHO to the atmosphere. This would result in a diel cycle consistent with the *Jacobi et al.* [2002] findings. To translate these flux values to volumetric fluxes, for use in our 0-D model, we assumed an appropriate atmospheric mixing height. At Summit, in July, potential temperature generally increases with altitude, a condition that inhibits convective mixing [*Helmig et al.*, 2002]; however, shortly after the short-wave radiation reaches its maximum value, unstable conditions can occur, as discussed by *Cullen and Steffen* [2002] for the Summit 2000 experiment. But, because the mixing time through the boundary layer can considerably exceed the lifetimes of photochemically active species, under all stability conditions, the concept of a "mixed layer" is inaccurate (e.g., for HCHO). In our model, we invoke the concept of "effective mixing height," defined as the vertical scale a particular species can diffuse over one lifetime. This calculation is time and species dependent, as it relies on the lifetime of the particular species and the eddy diffusivity. To simulate the impact of emission of these species using our model, we calculated a volumetric flux, $F_v = F_z/Z_i$, where Z is the effective mixing height for species i, i.e., $Z_i = (K_z\ \tau_i)^{1/2}$. For this calculation, we assume that an emitted species mixes vertically over a spatial scale equivalent to the distance it can diffuse in one lifetime [*Guimbaud et al.*, 2002]. Here τ_i is the calculated time varying atmospheric lifetime of species i, and Kz is the time-varying eddy diffusivity (the minimum lifetime is 1.1 hours for HCHO and 10.5 hours for H_2O_2 at 1245 local time). For this calculation, diurnally varying eddy diffusivity values (K_z) were determined for heights between two and four meters, as described

by *Honrath et al.* [2002]. The K_z values are shown in Figure 6, along with time varying lifetimes for HCHO and H_2O_2. A complication with this method is that the eddy diffusivity measurements may be underestimated, as we are using values obtained for two to four meters as representative of those over the full effective mixing height. Thus the calculated effective mixing heights may be low (or in other words, our volumetric input rates may be too large), since eddy diffusivities increase with altitude. Thus effective mixing heights used are lower limits, and the volumetric input rates are upper limit values. We calculated volumetric fluxes for HCHO and H_2O_2 from the time varying flux measurements of *Jacobi et al.* [2002], and using the calculated Z_i's, which are shown in Figure 7. The H_2O_2 flux was then included in our model as time varying, zero-dimensional emission and deposition rates, and the model output was determined with and without the HCHO flux. The resulting fluxes are plotted for both species in Figure 7, where positive numbers represent emission from the snowpack and negative numbers represent deposition. Also shown is the flux used by *Hutterli et al.* [1999] in their modeling, scaled to an average of 1.0×10^{13} molecules $m^{-2}\ sec^{-1}$ (with the same shape and deposition values as the *Jacobi et al.* [2002] flux) generated by multiplying the emission terms of the *Jacobi et al.* [2002] flux data by 11.6. This flux was then converted to a volumetric input rate based on our time varied effective mixing height. These two flux determinations, from which we calculated the volumetric fluxes required by our model, are the only two published determinations. Because of apparent interannual variability of fluxes (as seen from the large difference in magnitude between 1996 and 2000 flux measurements), we will examine each of the 2 years separately and compare the
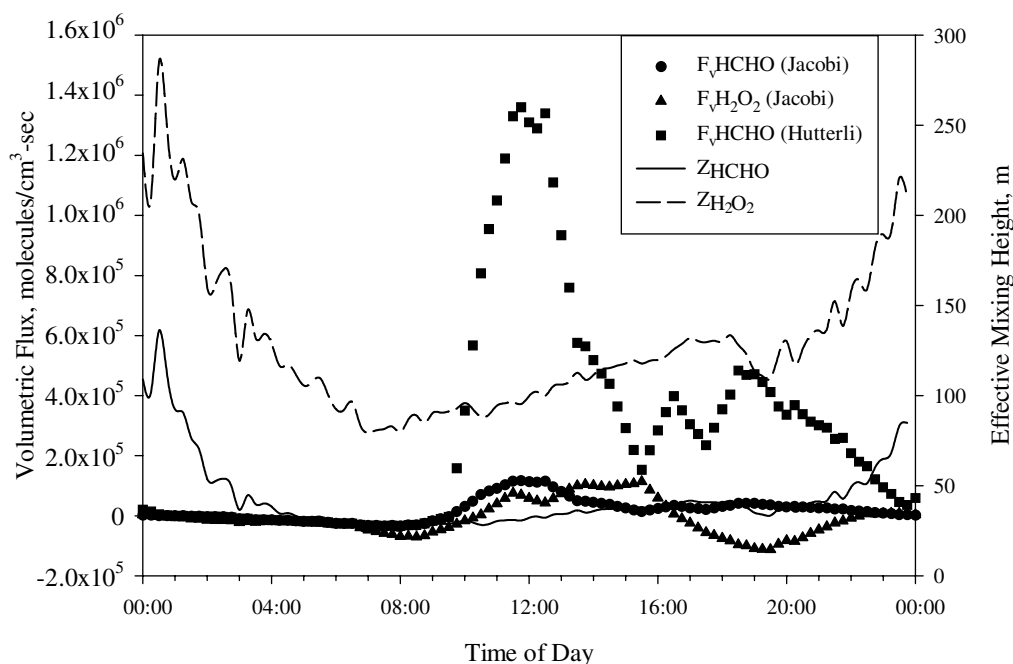
Figure 7. Diurnal variation of volumetric flux and mixing height. The two lines represent effective mixing height for HCHO (solid line) and H_2O_2 (dashed line). The symbols represent determinations of volumetric flux based upon the mixing heights plotted in this figure. The circles are the HCHO flux measured in 2000, the triangles are the H_2O_2 flux measured in 2000 [*Jacobi et al.*, 2002], and the squares are the HCHO flux used to model the 1996 field season [*Hutterli et al.*, 1999]. For the fluxes, positive numbers represent emission from the snowpack and negative numbers represent deposition.

model predictions to both the diurnal average for that year and to a representative day for each field campaign.

3.3.3. Case 1: Summer 2000

[27] Figure 8 (top) shows the model simulations and data for the 2000 field campaign, using the 2000 measured snowpack fluxes [*Jacobi et al.*, 2002]. 18 June 2000 was chosen as a representative day as it possesses a diel cycle consistent with the calculated average, has concentrations in the range of the majority of the data, and has good data coverage. Even without the addition of a flux, the model overestimates HCHO, as compared to the ambient data. When the 2000 flux is added, the simulated HCHO exhibits more of a diel cycle, maximizing right after noon and minimizing in the morning. This is inconsistent with the diel cycle observed in the ambient data, which shows a maximum in the morning, where the model predicts the lowest HCHO concentration, due to nighttime snowpack uptake. The addition of the flux also does not substantially increase HCHO concentration, but does contribute to the early afternoon peak. Between noon and 1300, the snowpack flux contribution to atmospheric HCHO production is 13%, with methane oxidation remaining the dominant HCHO precursor.

3.3.4. Case 2: Summer 1996

[28] As a first estimate of the HCHO flux for the 1996 campaign, we used the *Hutterli et al.* [1999] model flux value, 1.0×10^{13} molecules m^{-2} sec^{-1}, as an average flux for the month of June, scaled to the same diurnal profile found in 2000 and converted to a volumetric flux as before. Although *Hutterli et al.* [1999] did not detect or discuss a diurnally varying HCHO flux, since the *Jacobi et al.* [2002]

flux is similar in shape to the diel cycle of temperature, it is reasonable to assume that the flux profile is similar year-to-year. The model results and ambient data are shown in Figure 8 (bottom). 14 June 1996 was chosen as a representative day because it had good data coverage, no diel cycle (consistent with the results of *Hutterli et al.* [1999]) and had concentrations in the range of the majority of the data (although slightly smaller than the diurnal average concentrations). For 14 June 1996, the gas-phase base model does a good job of accounting for the ambient HCHO concentrations. However, adding the diurnally varying *Hutterli et al.* [1999] best estimate flux predicts much higher daytime concentrations of HCHO, specifically a noon maximum of ~400 ppt. Between noon and 1300, the model predicts a snowpack flux contribution to atmospheric HCHO production of 64%. At all other times of the day, gas-phase photochemical production is a more important source than is the snowpack. The model also predicts a large diel cycle for HCHO, maximizing right after noon. The magnitude of the maximum HCHO concentrations and the presence of a diurnal variation in HCHO are both inconsistent with the 1996 data. Interestingly, the model output is more consistent in shape with the data shown in Figure 2 for 1999 (i.e., HCHO maximizes right after noon).

[29] As a diurnally varying snowpack flux for HCHO was not specifically observed in 1996, we also applied the *Hutterli et al.* [1999] flux as a constant input for comparison. Thus in Figure 8, we also show the simulated HCHO using the *Hutterli et al.* [1999] average value as a constant flux (but varying volumetric input rate, due to the time
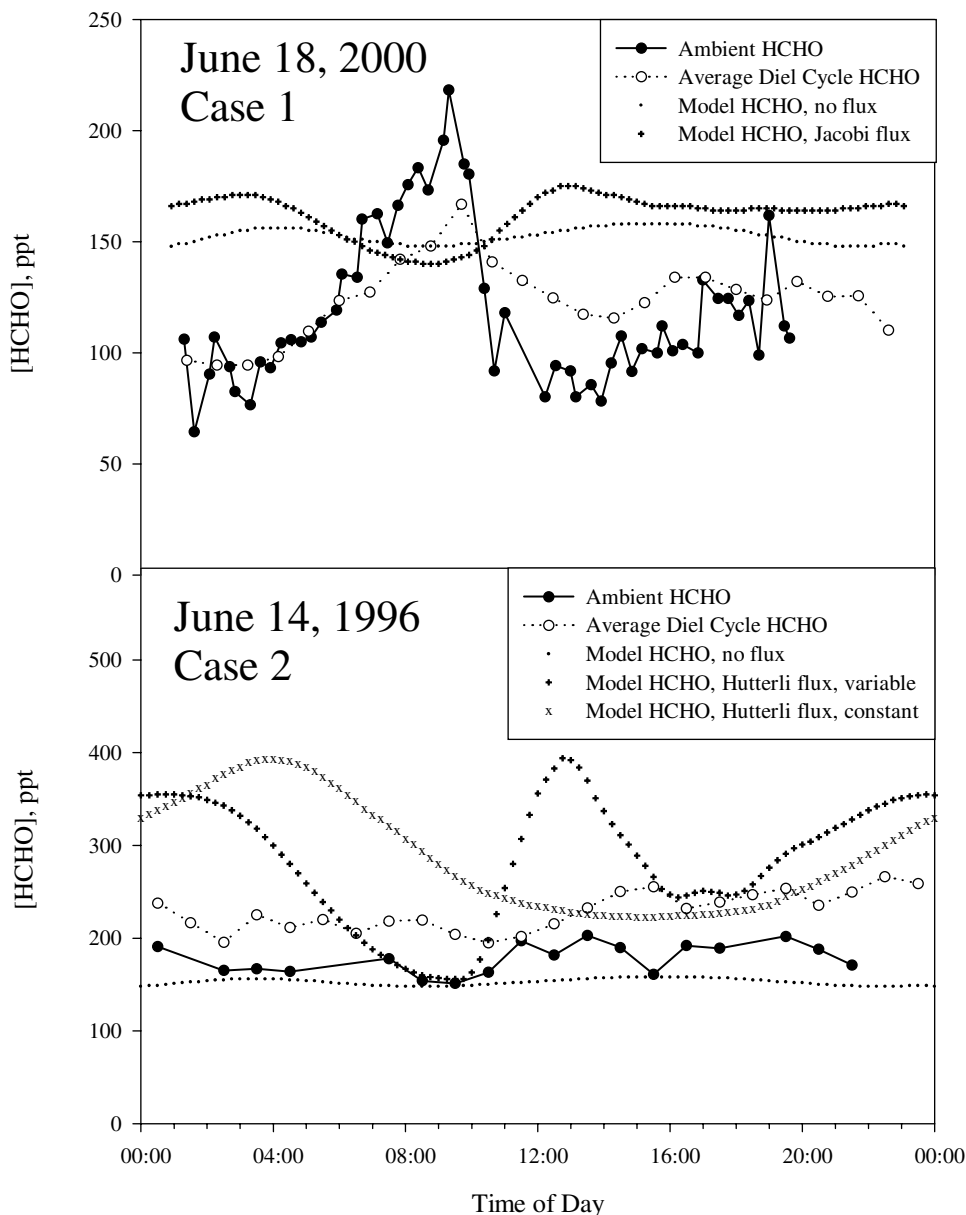
Figure 8. Comparison of measured and simulated HCHO for 2000 and 1996. Modeled HCHO is shown without a snowpack flux (small dots), with the *Jacobi et al.* [2002] flux (Case 1-2000, crosses), with the *Hutterli et al.* [1999] average flux scaled to the shape of the *Jacobi et al.* [2002] flux (Case 2-1996, crosses), and the *Hutterli et al.* [1999] average flux as a constant input (Case 2-1996, x symbols). Ambient data from representative days of each field campaign (solid circles) and the average diel cycle for each field campaign (open circles) are also shown.

varying effective mixing height). In both cases, the 24-hour integrated HCHO flux is the same. With this treatment, the model predicted a HCHO maximum of 400 ppt in the early morning, roughly twice that observed, and a broad minimum in the early afternoon. For both flux treatments, the early morning maximum predicted is inconsistent with the observations. For this simulation, the snowpack efflux contribution to atmospheric HCHO production between noon and 1300 is much lower, at 12%.

3.3.5. Discussion

[30] It is clear with these two cases that although the combination of gas-phase photochemistry and snowpack

flux can account for the average observed concentrations, our model does not capture the diel cycle in HCHO observed in some, but not all, of the data sets. Although we used the June average best estimate flux from the work of *Hutterli et al.* [1999], the actual calculated fluxes ranged from 1.4×10^{12} to 8.8×10^{12} molecules m^{-2} sec^{-1}, which were estimated from measurements of the concentrations gradient in the firn air. The *Jacobi et al.* [2002] diel average flux was 6.9×10^{11} molecules m^{-2} sec^{-1}, an order of magnitude smaller. If these two studies are correct, there must be a large interannual variability in HCHO flux. The flux of HCHO from the snowpack is dependent on both

temperature and snowpack HCHO concentration, as well as snow grain physical and chemical morphology. Comparing ambient temperature to HCHO concentration for all years shows no correlation between the two variables (within each measurement period). In addition, the average temperatures for all 5 years are similar, with a standard deviation of the average of 1.9°C. In fact, in 1996, temperature increased throughout the study (by ~15°C), and the gas-phase HCHO concentration did not correlate with this change. Surface snowpack HCHO concentrations for the 5 years compared here are also similar [*Fuhrer et al.*, 1996; *Hutterli et al.*, 1999; *Jacobi et al.*, 2002]. However, as discussed by *Hutterli et al.* [1999], assessment of the impact of desorption-driven flux requires knowledge of the vertical distribution of HCHO throughout the top ~1 meter of the snowpack. It is clear that much more flux measurement data is needed to enable quantitative and predictive understanding of the relationships between snowpack temperature, composition, radiation, and HCHO fluxes.

[31] The discrepancy between the observations and both model simulations imply that we do not yet fully understand gas-phase HCHO chemistry at Summit. Although it is possible that the snowpack HCHO flux is highly variable, it is also possible that we are missing a gas-phase photochemical source term. In support of this argument, *Singh et al.* [2001] reported large concentrations of oxygenated organic compounds in the remote troposphere. They found, among other compounds, high levels of methanol (~900 ppt) and methylhydroperoxide (~1 ppb; our model only predicts ~120 ppt), both of which are HCHO precursors. HCHO precursors, such as methylhydroperoxide, are in turn likely produced from oxidation of larger unidentified organic precursors, which could also produce HCHO directly. There is a wide range of potential sources; as an example, *Warneke et al.* [1999] reported that abiotic decay of biomass produces products such as HCHO, CH_3CHO, $CH_3C(O)CH_3$, and CH_3OH. If atmospheric particulate matter contains biosphere-derived components, heterogeneous oxidation (e.g., via O_3) of that organic particulate matter could be a possible HCHO source. A variety of large organic molecules can be oxidized to produce HCHO. It has been hypothesized that oxygenated VOCs can be produced by ozonolysis of unsaturated fatty acids incorporated in inverted micelle aerosols [*Ellison et al.*, 1999]. This could allow for the transport of carbonyl compound precursors to remote environments and the free troposphere, such as Summit. Our snowpack analytical data make it clear that we do not understand the sources of organic carbon to the Summit surface. Thus, there is a great need for analytical work with respect to the organic composition in both the gas and the snowpack phases.

4. Conclusions

[32] The model simulations of ambient HCHO using 1996 and 2000 HCHO flux measurement data show conflicting results that do not simulate (and often underpredict) ambient concentrations. The firn air experiment described here indicates that HCHO can be photochemically produced in the snowpack. However, the importance of this to the flux, and the snowpack and ambient HCHO concentrations

is as yet unclear. The result for HCHO can now be taken in the context of recent reports of HCHO, CH_3CHO, and acetone production in the snowpack at Alert [*Guimbaud et al.*, 2002; *Grannas et al.*, 2002; *Boudries et al.*, 2002; *Sumner et al.*, 2002], as well as production of alkyl halides and alkenes at Summit [*Swanson et al.*, 2002], and CO production in Alpine snow [*Haan et al.*, 2001]. Indeed, it is very interesting that *Haan et al.* [2001] show that CO photoproduction is well correlated with snowpack TOC levels, and conclude that HCHO is likely a CO precursor. The *Swanson et al.* [2002] report makes it clear that the sunlit snowpack exhibits active and interesting organic photochemistry. In order to understand the production of HCHO in the snowpack, additional research into the nature of its precursors in the snowpack must be conducted. It is also clearly necessary to better quantify and understand environmental variables that influence the HCHO flux from the snowpack.

References

Atkinson, R., D. L. Baulch, R. A. Cox, R. F. Hampson, J. A. Kerr, M. J. Rossi, and J. Troe, Evaluated kinetic and photochemical data for atmospheric chemistry: Supplement VI, *J. Phys. Chem. Ref. Data*, *26*, 1329–1499, 1997.

Atkinson, R., D. L. Baulch, R. A. Cox, R. F. Hampson, J. A. Kerr, M. J. Rossi, and J. Troe, Evaluated kinetic and photochemical data for atmospheric chemistry, organic species: Supplement VII, *J. Phys. Chem. Ref. Data*, *28*, 191–393, 1999.

Boudries, H., J. W. Bottenheim, C. Guimbaud, A. Grannas, P. B. Shepson, S. Houdier, S. Perrier, and F. Domine, Distribution and trends of oxygenated hydrocarbons in the high Arctic derived from measurements in the atmospheric boundary layer and interstital snow air during the ALERT 2000 field campaign, Alert 2000, *Atmos. Environ.*, *36*, 2573–2583, 2002.

Burkhart, J. F., M. Hutterli, and R. C. Bales, Partitioning of formaldehyde between air and ice at −35°C to −5°C, *Atmos. Environ.*, in press, 2002.

Calace, N., B. M. Petronio, R. Cini, A. M. Stortini, B. Pampaloni, and R. Udisti, Humic marine matter and insoluble materials in Antarctic snow, *Int. J. Environ. Anal. Chem.*, *79*, 331–348, 2001.

Couch, T. L., A. L. Sumner, T. M. Dassau, P. B. Shepson, and R. E. Honrath, An investigation of the interaction of carbonyl compounds with the snowpack, *Geophys. Res. Lett.*, *27*, 2241–2244, 2000.

Cincinelli, A., P. G. Desderi, L. Lepri, L. Checchini, M. Del Bubba, and R. Udisti, Marine contribution to the chemical composition of coastal and inland Antarctic snow, *Int. J. Environ. Anal. Chem.*, *74*, 283–299, 2001.

Cullen, N., and K. Steffen, Unstable near-surface boundary conditions in summer on top of the Greenland ice sheet, *Geophys. Res. Lett.*, *28*, 4491–4492, 2002.

DeMore, W. B., S. P. Sander, D. M. Golden, R. F. Hampson, M. J. Kurylo, C. J. Howard, A. R. Ravishankara, C. E. Kolb, and M. J. Molina, Chemical kinetics and photochemical data for use in stratospheric modeling: Evaluation number 12, *JPL Publ. 97-4*, 1–266, 1997.

Desderi, P. G., L. Lepri, R. Udisti, L. Checchini, M. Del Bubba, R. Cini, and A. Stortini, Analysis of organic compounds in Antarctic snow and their origin, *Int. J. Environ. Anal. Chem.*, *71*, 331–351, 1998.

Dibb, J. E., M. Arsenault, M. C. Peterson, and R. E. Honrath, Fast nitrogen oxide photochemistry in Summit, Greenland snow, *Atmos. Environ.*, *36*, 2501–2511, 2002.

Ellison, G. B., A. F. Tuck, and V. Vaida, Atmospheric processing of organic aerosols, *J. Geophys. Res.*, *104*, 11,633–11,641, 1999.

Fan, Q., and P. K. Dasgupta, Continuous automated determination of atmospheric formaldehyde at the parts per trillion level, *Anal. Chem.*, *66*, 551–556, 1994.

Fuhrer, K., M. Hutterli, and J. R. McConnell, Overview of recent field experiments for the study of the air-snow transfer of H_2O_2 and HCHO, in *Chemical Exchange Between the Atmosphere and Polar Snow*, NATO ASI, pp. 307–318, Springer-Verlag, New York, 1996.

Grannas, A. M., et al., Carbonyl compounds and surface photochemistry in the arctic marine boundary layer, *Atmos. Environ.*, *36*, 2733–2742, 2002.

Grollert, C., and H. Puxbaum, Lipid organic aerosol and snow composition at a high alpine site in the fall and the spring season and scavenging ratios for single compounds, *Water Air Soil Pollut.*, *117*, 157–173, 2000.

Guimbaud, C., et al., Snowpack processing of acetaldehyde and acetone in the Arctic atmospheric boundary layer, *Atmos. Environ.*, *36*, 2743–2752, 2002.

Haan, D., and D. Raynaud, Ice core record of CO variations during the last two millennia: Atmospheric implications and chemical interactions within the Greenland ice, *Tellus*, *50B*, 253–262, 1998.

Haan, D., Y. Zuo, V. Gros, and A. M. Brenninkmeijer, Photochemical production of carbon monoxide in snow, *J. Atmos. Chem.*, *40*, 217–230, 2001.

Helmig, D., J. Boulter, D. David, J. Birks, N. Cullen, K. Steffen, B. Johnson, and S. Oltmans, Ozone and meteorological boundary-layer conditions at Summit, Greenland during 3–21 June 2000, *Atmos. Environ.*, *36*, 2595–2608, 2002.

Honrath, R. E., M. C. Peterson, S. Guo, J. E. Dibb, P. B. Shepson, and B. Campbell, Evidence of NO_x production and release within the snowpack at Summit, Greenland, *Geophys. Res. Lett.*, *26*, 695–698, 1999.

Honrath, R. E., S. Guo, M. C. Peterson, M. P. Dziobak, J. E. Dibb, and M. A. Arsenault, Photochemical production of gas phase NO_x from ice crystal NO_3^-, *J. Geophys. Res.*, *105*, 24,183–24,190, 2000.

Honrath, R. E., Y. Lu, M. C. Peterson, J. E. Dibb, M. A. Arsenault, N. J. Cullen, and K. Steffen, Vertical fluxes of NO_x, HONO, and HNO_3 above the snowpack at Summit, Greenland, *Atmos. Environ.*, *36*, 2629–2640, 2002.

Houdier, S., S. Perrier, F. Domine, A. Cabanes, L. Legagneux, A. M. Grannas, C. Guimbaud, P. B. Shepson, H. Boudries, and J. W. Bottenheim, Acetaldehyde and acetone in the Arctic snowpack during the ALERT2000 field campaign: Snowpack composition, incorporation processes and atmospheric impact, *Atmos. Environ.*, *36*, 2609–2618, 2002.

Hutterli, M. A., R. Rothlisberger, and R. C. Bales, Atmosphere-to-snow-to-firn transfer studies of HCHO at Summit, Greenland, *Geophys. Res. Lett.*, *26*, 1691–1694, 1999.

Jacobi, H. W., M. M. Frey, M. A. Hutterli, R. C. Bales, O. Schrems, N. J. Cullen, K. Steffen, and C. Koehler, Measurements of hydrogen peroxide and formaldehyde exchange between the atmosphere and surface snow at Summit, Greenland, *Atmos. Environ.*, *36*, 2619–2628, 2002.

Jaegle, L., D. J. Jacob, W. H. Brune, and P. O. Wennberg, Chemistry of HO_x radicals in the upper troposphere, *Atmos. Environ.*, *35*, 469–489, 2001.

Keiber, R. J., and K. Mopper, Determination of picomolar concentrations of carbonyl compounds in natural waters, including seawater, by liquid chromatography, *Environ. Sci. Technol.*, *24*, 1477–1481, 1990.

King, M. D., and W. R. Simpson, Extinction of UV radiation in Arctic snow at Alert, Canada (82 degrees N), *J. Geophys. Res.*, *106*, 12,499–12,507, 2001.

Li, J., P. K. Dasgupta, Z. Genfa, and M. A. Hutterli, Measurement of atmospheric formaldehyde with a diffusion scrubber and light-emitting diode: Liquid-core waveguide based fluorometry, *Field Anal. Chem. Technol.*, *5*, 2–12, 2001.

MacDonald, A. M., et al., Results of a formaldehyde intercomparison study in Ontario, paper presented at Am. Geophys. Union Fall Meet., San Francisco, Calif., 6–12 December 1998.

Michalowski, B., J. S. Francisco, Y. Li, S. M. Li, and P. B. Shepson, A study of multiphase chemistry in the Arctic boundary layer during polar sunrise, *J. Geophys. Res.*, *105*, 15,131–15,145, 2000.

Neftel, A., R. C. Bales, and D. J. Jacob, H_2O_2 and HCHO in polar snow and their relation to atmospheric chemistry, in *Ice Core Studies of Global Biogeochemical Cycles*, NATO ASI, pp. 249–264, Springer-Verlag, New York, 1995.

Perrier, S., S. Houdier, F. Domine, A. Cabanes, L. Legagneux, A. L. Sumner, and P. B. Shepson, Formaldehyde in Arctic snow. Incorporation into ice particles and evolution in the snowpack, *Atmos. Environ.*, *36*, 2695–2705, 2002.

Peterson, M., D. Barber, and S. Green, Monte Carlo modeling and measurement of actinic flux levels in Summit, Greenland snowpack, *Atmos. Environ.*, *36*, 2541–2551, 2002.

Sehested, J., L. K. Christensen, O. J. Nielsen, M. Bilde, T. J. Wallington, W. F. Schneider, J. J. Orlando, and G. S. Tyndall, Atmospheric chemistry of acetone: Kinetic study of the $CH_3C(O)CH_2O_2$ + NO/NO_2 reactions and decomposition of $CH_3C(O)CH_2O_2NO_2$, *Int. J. Chem. Kinet.*, *30*, 475–489, 1998.

Shepson, P. B., A. P. Sirju, J. F. Hopper, L. A. Barrie, V. Young, H. Niki, and H. Dryfhout, Sources and sinks of carbonyl compounds in the Arctic Ocean boundary layer: Polar Ice Floe Experiment, *J. Geophys. Res.*, *101*, 21,081–21,089, 1996.

Simpson, W. R., M. D. King, H. J. Beine, R. E. Honrath, and X. Zhou, Radiation-transfer modeling of snowpack photochemical processes during ALERT 2000, *Atmos. Environ.*, in press, 2002.

Singh, H., Y. Chen, A. Staudt, D. Jacob, D. Blake, B. Heikes, and J. Snow, Evidence from the Pacific troposphere for large global sources of oxygenated organic compounds, *Nature*, *410*, 1078–1081, 2001.

Sirju, A. P., and P. B. Shepson, A laboratory and field investigation of the DNPH cartridge technique for the measurement of atmospheric carbonyl compounds, *Environ. Sci. Technol.*, *29*, 384–392, 1995.

Staffelbach, T., A. Neftel, B. Stauffer, and D. Jacob, A record of the atmospheric methane sink from formaldehyde in polar ice cores, *Nature*, *349*, 603–605, 1991.

Staffelbach, T., et al., Photochemical oxidant formation over southern Switzerland: Results from summer 1994, *J. Geophys. Res.*, *102*, 23,345–23,362, 1997.

Stauffer, B., Long term climate records from polar ice, *Space Sci. Rev.*, *94*, 321–336, 2000.

Sumner, A. L., The role of formaldehyde in tropospheric ozone chemistry, Ph.D. Thesis, Purdue Univ., West Lafayette, IN, 2001.

Sumner, A. L., and P. B. Shepson, Snowpack production of formaldehyde and its effect on the Arctic troposphere, *Nature*, *398*, 230–233, 1999.

Sumner, A. L., et al., Atmospheric chemistry of formaldehyde in the Arctic troposphere at Polar Sunrise, and the influence of the snowpack, *Atmos. Environ.*, *36*, 2553–2562, 2002.

Swanson, A. L., N. J. Blake, J. E. Dibb, M. R. Albert, D. R. Blake, and F. S. Rowland, Photochemically induced production of CH_3Br, CH_3I, C_2H_5I, ethene, and propene within surface snow, *Atmos. Environ.*, *36*, 2671–2682, 2002.

Thompson, A. M., The oxidizing capacity of the Earth's atmosphere: Probably past and future changes, *Science*, *256*, 1157–1165, 1995.

Twickler, M. S., M. J. Spencer, W. B. Lyons, and P. A. Mayewski, Measurement of organic carbon in polar snow samples, *Nature*, *320*, 156–158, 1986.

Villenave, E., and R. Lesclaux, Kinetics of the cross reactions of CH_3O_2 and $C_2H_5O_2$ radicals with selected peroxy radicals, *J. Phys. Chem.*, *100*, 14,372–14,388, 1996.

Walker, J. F., *Formaldehyde*, 3rd edition, Van Nostrand Reinhold, New York, 1964.

Warneke, C., T. Karl, H. Judmaier, A. Hansel, A. Jordan, and W. Lindinger, Acetone, methanol, and other partially oxidized volatile organic emissions from dead plant matter by abiological processes: Significance for atmospheric HO_x chemistry, *Glob. Biogeochem. Cycles*, *13*, 9–17, 1999.

Yang, C., P. A. Mayewski, M. S. Twickler, and S. Whitlow, Major features of glaciochemistry over the last 110,000 years in the Greenland Ice Sheet Project 2 ice core, *J. Geophys. Res.*, *102*, 23,289–23,299, 1997.

Yang, J., R. E. Honrath, M. C. Peterson, J. E. Dibb, A. L. Sumner, P. B. Shepson, M. Frey, H. W. Jacobi, A. Swanson, and N. Blake, Impacts of snowpack emissions on deduced levels of OH and peroxy radicals at Summit, Greenland, *Atmos. Environ.*, *36*, 2523–2534, 2002.

Zhou, X., and K. Mopper, Photochemical production of low-molecular-weight carbonyl compounds in seawater and surface microlayer and their air–sea exchange, *Mar. Chem.*, *56*, 201–213, 1997.

———————————

T. M. Dassau, S. L. Koeniger, P. B. Shepson, and A. L. Sumner, Department of Chemistry, Purdue University, West Lafayette, IN, USA. (terra@highstream.net)

R. E. Honrath and J. Yang, Department of Civil and Environmental Engineering, Michigan Technological University, Houghton, MI, USA.

N. J. Cullen and K. Steffen, Cooperative Institute for Research in Environmental Sciences, University of Colorado, Boulder, CO, USA.

R. C. Bales, M. Frey, and H.-W. Jacobi, Department of Hydrology and Water Resources, University of Arizona, Tucson, AZ, USA.